arXiv:0903.1026v2 [cond-mat.soft] 15 Mar 2009

Molecular Dynamics Simulation of Semiflexible Polyampholyte Brushes - The Effect of Charged Monomers Sequence

M. Baratlo and H. Fazli*
Institute for Advanced Studies in Basic Sciences (IASBS), P. O. Box 45195-1159, Zanjan 45195, Iran

(Dated: March 15, 2009)

Planar brushes formed by end-grafted semiflexible polyampholyte chains, each chain containing equal number of positively and negatively charged monomers is studied using molecular dynamics simulations. Keeping the length of the chains fixed, dependence of the average brush thickness and equilibrium statistics of the brush conformations on the grafting density and the salt concentration are obtained with various sequences of charged monomers. When similarly charged monomers of the chains are arranged in longer blocks, the average brush thickness is smaller and dependence of brush properties on the grafting density and the salt concentration is stronger. With such long blocks of similarly charged monomers, the anchored chains bond to each other in the vicinity of the grafting surface at low grafting densities and buckle toward the grafting surface at high grafting densities.

PACS numbers:

I. INTRODUCTION

Polymers carrying ionizable groups dissolved in a polar solvent dissociate into charged polymer chains and counter-ions (ions of opposite charge). Depending on acidic or basic property of ionizable monomers, charged polymers can be classified into polyelectrolytes containing a single sign of charged monomers and polyampholytes bearing both positive and negative charges. These macromolecules are often water-soluble and have numerous applications in industry and medicine. Many biological macromolecules such as DNA, RNA, and proteins are charged polymers.

Charged monomers of different sign can be distributed randomly along a polyampholyte chain or charges of one sign can be arranged in long blocks. With excess of one type of charges, polyampholyte solutions exhibit properties similar to those of polyelectrolyte solutions. With the same ratio of positive and negative charges on the chains, the solution behavior depends noticeably on the charge sequence. For example, it has been shown that the sequence of charged amino acids (charge distribution) along ionically complementary peptides affect the aggregation behavior and self-assembling process in the solution of such peptides [1, 2]. Also, using Monte Carlo simulations it has been shown that charged monomers sequence of neutral block-polyampholytes affect their adsorption properties to a charged surface [3].

The present understanding of, in particular, random polyampholytes in solution and their interaction with surfaces and polyelectrolytes has recently been reviewed [4]. In addition, theoretical and computer simulation studies of single diblock polyampholytes [5, 6, 7], and diblock polyampholytes in solution [8, 9], have been performed. The value of salt concentration in the solution is an important parameter for tuning the structural properties of polyampholyte chains. With increasing the salt concentration, the coil size and the viscosity increase in the solution of nearly charge-balanced polyampholyte chains and decrease in the case of the solution of polyampholytes with a large net charge (the polyelectrolyte regime)[10, 11, 12, 13].

The properties of the system of polymers anchored on a surface are of great interest both in industrial and biological applications and academic research. When there is sufficiently strong repulsion between the polymers, the chains become stretched and the structure obtained is known as a polymer brush. Brushes at planar and curved surfaces formed by grafted homopolymers have extensively been investigated by various theoretical methods [14, 15, 16, 17].

In the case of polyelectrolytes grafted onto a surface (polyelectrolyte brush), the repulsion of electrostatic origin between the chains can be considerable even at low grafting densities, making it easy the system to access the brush regime. The use of charged polymers instead of uncharged polymers introduces additional length scales

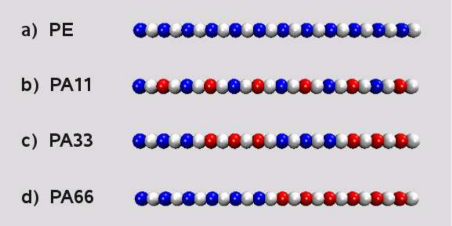

FIG. 1: (Color online) Schematic structures of four different chains containing different sequences of charged monomers. Neutral, positively and negatively charged monomers are shown by white, red (dark) and blue (black) spheres respectively. The chain containing only negatively charged monomers is a polyelectrolyte chain, PE, and three other chains PA11, PA33 and PA66 are polyampholytes consisting of alternating blocks of similarly charged monomers with 1, 3 and 6 monomers in each block respectively.

---

*Electronic address: fazli@iasbs.ac.ir

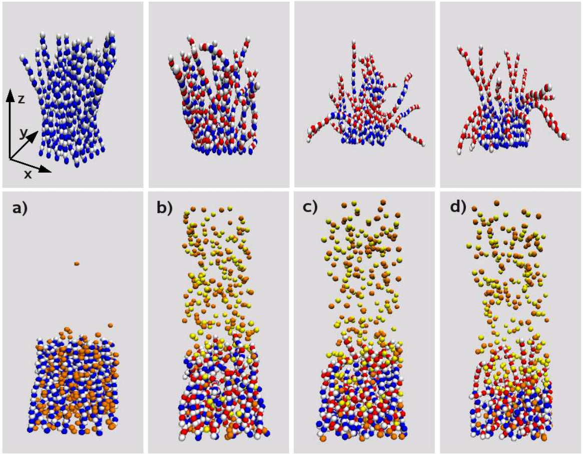

FIG. 2: (Color online) Typical equilibrium configurations of brushes formed by a)PE, b)PA11, c)PA33, and d)PA66 chains at grafting density $\rho_a\sigma^2 = 0.1$. In the upper plans, counterions are not shown and periodic boundary condition is removed for clarity. As it can be seen, in the brushes of PA33 and PA66, the chains are buckled toward the grafting surface.

such as Bjerrum length and Debye screening length to the system. Polyelectrolyte brushes also have been subjected to extensive investigations involving both theoretical [18, 19, 20, 21, 22, 23, 24, 25] and computer simulation methods [23, 24, 25, 26, 27, 28]. At high enough grafting densities and charge fractions of polyelectrolyte chains, most of counterions are trapped inside the polyelectrolyte brush and competition between osmotic pressure of the counterions and elasticity of the chains determines the brush thickness. This regime of a polyelectrolyte brush is known as the osmotic regime in which some theoretical scaling methods predict no dependence of the brush thickness to the grafting density [18, 29]. However, other scaling method that takes into account the excluded volume effects and nonlinear elasticity of polyelectrolyte chains predicts a linear dependence of the brush thickness on the grafting density and is in agreement with experiment and simulation [23, 24, 25]. Also, it has been shown that diffusion of a fraction of counterions outside the polyelectrolyte brush leads to a logarithmic dependence of the average brush thickness on the grafting density [22].

Brushes formed by grafted diblock polyampholytes have also been investigated by lattice mean field modeling [30, 31] and computer simulation [32]. The effect of chain stiffness, charge density, and grafting density on spherical brushes of diblock polyampholytes and interaction between colloids with grafted diblock polyampholytes have been studied using Monte Carlo simulations [33, 34]. Despite the case of an osmotic polyelectrolyte brush that counterions are trapped inside the brush and have a crucial rule in the equilibrium brush thickness, in the case of a polyampholyte brush most of counterions are outside and equilibrium brush thickness is mainly determined by the chains properties.

A brush of semiflexible charged polymers is a dense assembly of such polymers in which the interplay between electrostatic correlations, entropic effects and the bending elasticity of the chains can bring about a variety of equilibrium properties. The strength of the electrostatic correlations in a polyampholyte brush depends on the sequence of charged monomers along the chains. With similarly charged monomers being arranged in long blocks, the electrostatic correlations are of great importance in the system. It seems that for a brush formed by semiflexible polyampholyte chains, each chain containing equal number of positive and negative monomers, studying the effect of monomers sequence on equilibrium properties of the brush could be an step toward better understanding of such system s.

In this paper, we study planar brushes of semiflexible polyampholytes using extensive molecular dynamics (MD) simulations in a wide range of the grafting density and at various salt concentrations. In our simulations, each end-grafted polyampholyte chain contains equal number of positively and negatively charged monomers (isoelectric condition). We investigate the effect of the sequence of charged monomers along the chains on equilibrium properties of the brush. Charged monomers of each sign are arranged in blocks of equal length and monomers of opposite sign form regular alternation of positive and negative blocks (see Fig. 1 b, c and d). Different charge sequences in our simulations correspond to different lengths of above mentioned blocks. We also consider the case of polyelectrolyte brush in our studies in which all the charged monomers of the chains are of the same sign for comparison.

We find that at each value of the grafting density, the brush formed by polyampholytes with longer blocks of similarly charged monomers has smaller average thickness, i.e., the lowest value of the average thickness corresponds to the brush of diblock polyampholytes. The values of the grafting density that we use in our simulations correspond to the osmotic regime of the polyelectrolyte brush. In this regime, most of the counterions are contained inside the polyelectrolyte brush and the average brush thickness has a weak linear dependence on the grafting density. Dependence of the average thickness of polyelectrolyte brush that we obtain from our simulations is in agreement with nonlinear theory of ref. [23]. In the case of the polyampholyte brush, we find that the average thickness considerably varies as a function of the grafting density and with longer blocks of similarly charged monomers, this dependence is stronger. Counterions of a polyampholyte brush are not trapped inside the brush and dependence of the average thickness on the grafting density originates from a different mechanism than that of a polyelectrolyte brush (see the text). We also study the equilibrium statistics of conformations of the chains at various grafting densities and salt concentrations both for polyampholyte and polyelectrolyte brushes. We find that in the case of polyampholyte

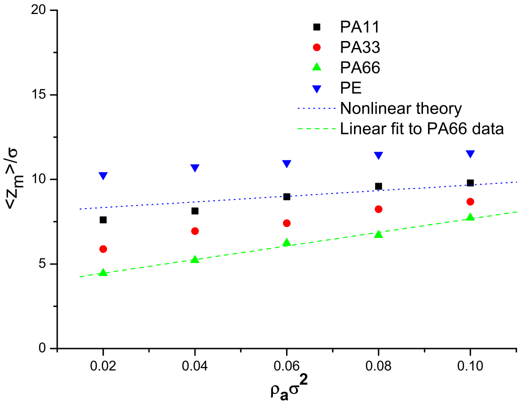

FIG. 3: (Color online) Average thickness of brushes formed by PE, PA11, PA33 and PA66 chains versus dimensionless grafting density $\rho_a\sigma^2$ with no added salt. Dotted line is the prediction of the scaling theory of ref. [23] with $\sigma_{eff} \simeq 1.02\sigma$ and dashed line is a linear fit to our data for the brush of PA66 chains. As it can be seen dependence of the average thickness of polyampholyte brushes with longer blocks of similarly charged monomers on the grafting density is stronger. The size of the symbols corresponds to the size of error bars.

brushes with long blocks of similarly charged monomers, at low grafting densities the inter-chain electrostatic interactions link the chains to each other in the vicinity of the grafting surface and cause the brush to collapse. At high grafting densities, although the excluded volume interactions tend to increase the brush thickness, the electrostatic interaction dominate over the bending elasticity of the chains and lead them to buckle and the brush thickness to decrease. Also it is observed that with long blocks of similarly charged monomers along the chains, the average thickness of the polyampholyte brush is an increasing function of the salt concentration.

The rest of the paper is organized as follows. In Sec. II we describe our model and details of molecular dynamics simulations. We present results of the simulations in detail and concluding remarks in Sec. III. Finally, in Sec. V we summarize the paper.

II. THE MODEL AND THE SIMULATION METHOD

In our simulations which are performed with the MD simulation package ESPResSo [35], each brush is modeled by M semiflexible polyelectrolyte/polyampholyte bead-spring chains of length N (N spherical monomers) which are end-grafted onto an uncharged surface at $z = 0$. Short-range repulsive interaction which is described by a shifted Lennard-Jones potential,

$$u_{LJ}(r) = \begin{cases} 4\varepsilon \left\{(\frac{\sigma}{r})^{12} - (\frac{\sigma}{r})^{6} + \frac{1}{4}\right\} & \text{if } r < r_c, \\ 0 & \text{if } r \geq r_c, \end{cases} \qquad (1)$$

is considered between monomers in which ϵ and σ are the usual Lennard-Jones parameters and the cutoff radius is $r_c = 2^{1/6}\sigma$. Neighboring beads along each chain are bonded to each other by a FENE (finite extensible nonlinear elastic) potential [36],

$$u_{bond}(r) = \begin{cases} -\frac{1}{2}k_{bond}R_0^2 \ln(1 - (\frac{r}{R_0})^2) & \text{if } r < R_0, \\ 0 & \text{if } r \geq R_0, \end{cases} \qquad (2)$$

with bond strength $k_{bond} = 30\varepsilon/\sigma^2$ and maximum bond length $R_0 = 1.5\sigma$. The chains are semiflexible and their elasticity is modeled by a bond angle potential,

$$u_{bend}(r) = k_{bend}(1 - \cos\theta), \qquad (3)$$

in which θ is the angle between two successive bond vectors of a chain. In our simulations $k_{bend} = 25k_BT$ which means that $l_p = 25\sigma \simeq L_c$ in which l_p and L_c are the persistence length and the contour length of the chains respectively. The simulation box is of volume $L \times L \times L_z$ in which L is the box width in x and y directions and L_z is its height in z direction and the grafting density is given by $\rho_a = M/L^2$. The positions of anchored monomers which are fixed during the simulation, form an square lattice with lattice spacing $d = \rho_a^{-1/2}$ on the grafting surface ($x - y$ plane). All particles interact repulsively with the grafting surface at short distances with the shifted Lennard-Jones potential introduced in Eq. 1. In addition, a similar repulsive potential is applied at the top boundary of the simulation box and in our simulations $L_z = 2N\sigma$. We model positive and negative ions of monovalent salt by equal number of spherical Lennard-Jones particles of diameter σ with charges e and $-e$ respectively. All the charged particles interact with the Coulomb interaction

$$u_C(r) = k_BTq_iq_j\frac{l_B}{r} \qquad (4)$$

in which q_i and q_j are charges of particles i and j in units of elementary charge e and r is separation between them. The Bjerrum length, l_B, which determines the strength of the Coulomb interaction relative to the thermal energy, k_BT, is given by $l_B = e^2/\varepsilon k_BT$, where ε is the dielectric constant of the solvent. $l_B = 2\sigma$ in our simulations. We apply periodic boundary conditions only in two dimensions (x and y). To calculate Coulomb forces and energies, we use the so-called MMM technique introduced by Strebel and Sperb [37] and modified for laterally periodic systems ($MMM2D$) by Arnold and Holm [38]. The temperature in our simulations is kept fixed at $k_BT = 1.2\varepsilon$ using a Langevin thermostat.

In our simulations we consider brushes containing $M = 25$ anchored chains, each chain consisting of $N = 24$ monomers, fN of them are charged and $f = \frac{1}{2}$. We also consider $\frac{M \times N}{2}$ counterions to neutralize the chains charge. The following sequences of charged monomers along the chains are considered to model polyelectrolyte

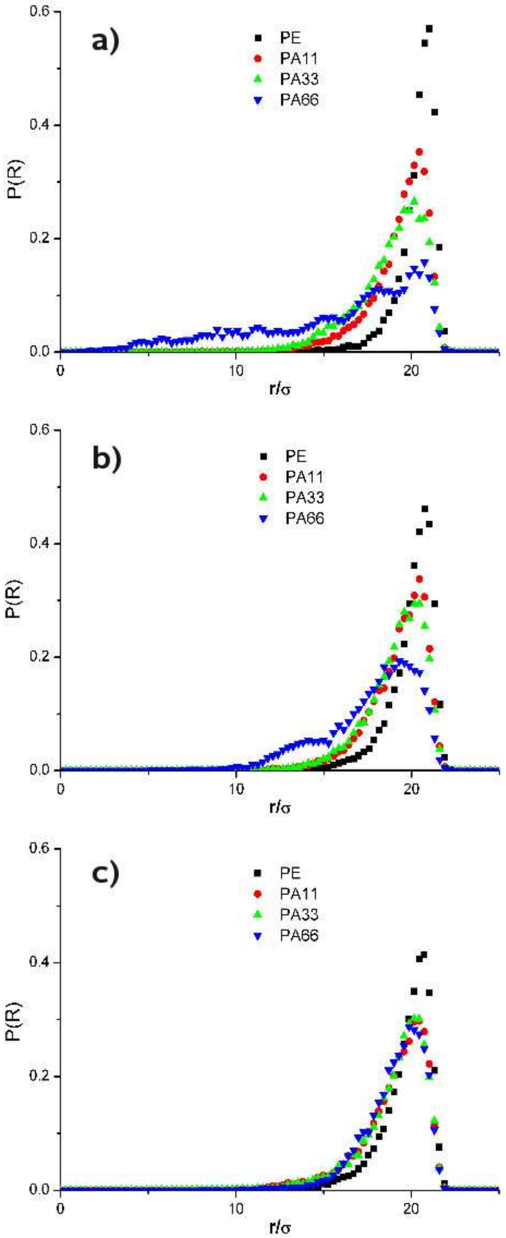

FIG. 4: The histogram of the average end-to-end distance of the chains for brushes formed by PE, PA11, PA33 and PA66 chains at grafting densities a) $\rho_a\sigma^2 = 0.1$, b)$\rho_a\sigma^2 = 0.06$ and c) $\rho_a\sigma^2 = 0.02$.

and three different polyampholyte brushes respectively: PE (...- - - - - ...) PA11 (...+ - + - + - ...), PA33 (...+ + + - - - ...)and PA66 (...+ + + + + + - - - - - - - ...). Each chain consist of an alternating sequence of charged and neutral monomers and the neutral monomers are not shown for simplicity (see Fig. 1). We do simulations of the brushes formed by four above mentioned different chains at dimensionless grafting densities $\rho_a\sigma^2 = 0.02, 0.04, 0.06, 0.08, 0.10$ and at various monovalent salt concentrations changing from $c_s\sigma^3 = 0$ to $c_s\sigma^3 = 0.22$. In the beginning of each simulation, all of the chains are straight and perpendicular to the grafting surface and all the ions are randomly distributed inside the simulation box. We equilibrate the system for 1.6×10^6 MD time steps which is enough for all values of the grafting density mentioned above and then calculate thermal averages over 1500 independent configurations of the system selected from 2.25×10^6 additional MD steps after equilibration. MD time step in our simulations is $\tau = 0.01\tau_0$ in which $\tau_0 = \sqrt{\frac{m\sigma^2}{\varepsilon}}$ is the MD time scale and m is the mass of the particles.

We calculate the average brush thickness which can be measured by taking the first moment of the monomer density profile

$$\langle z_m \rangle = \frac{\int_0^\infty z\rho_m(z)dz}{\int_0^\infty \rho_m(z)dz}, \tag{5}$$

in which $\rho_m(z)$ is the number density of monomers as a function of the distance from the grafting surface. For better understanding of the statistics of the chains conformations, we calculate the histogram of the mean end-to-end distance of the chains, $P(R)$, in which $R = \frac{1}{M}\sum_{i=1}^{M} |\vec{R}_i|$ and $\vec{R}_i$ is the end-to-end vector of chain i. We also calculate the histogram of the average distance of the end monomers of the chains from the grafting surface, $P(z_{end})$, in which $z_{end} = \frac{1}{M}\sum_{i=1}^{M} z_i$ and z_i is the z component of the end monomer of chain i. Also, as a measure of the lateral fluctuations of the chains we define l_{lat} as $l_{lat} = \frac{1}{M}\sum_{i=1}^{M} R_{i||}$ in which $R_{i||} = |\vec{R}_i - \vec{R}_i.\vec{\hat{z}}|$ is the magnitude of the lateral component of $\vec{R}_i$.

III. RESULTS AND CONCLUDING REMARKS

We calculate the average thickness of the brushes formed by polyelectrolyte chain, PE, and three different polyampholyte chains PA11, PA33 and PA66 at different grafting densities. In Fig. 3 the average brush thickness versus dimensionless grafting density $\rho_a\sigma^2$ with no added salt is shown. As it can be seen in this figure, the average thickness of the polyelectrolyte brush has a week dependence on the grafting density. With grafting densities that we use in our simulations, the Gouy-Chapman length of the polyelectrolyte brush which is defined as $\lambda_G = (2\pi\rho_a f N l_B)^{-1}$, is quite smaller than the length of the chains ($\lambda_G < \sigma$) and most of the counterions are contained inside the brush (see Fig. 1 a). In this regime of polyelectrolyte brushes, the osmotic pressure of the counterions determines the thickness of the brush and the week dependence of the brush thickness on the grafting density is expected. In fig. 3 the prediction of the scaling theory of ref. [23] (see Eq. (28) of [23]) corresponding to our parameters is shown for comparison. As it can be seen, this scaling theory describes well the dependence of the average thickness of semiflexible osmotic polyelectrolyte brush on the grafting density obtained from our simulations.

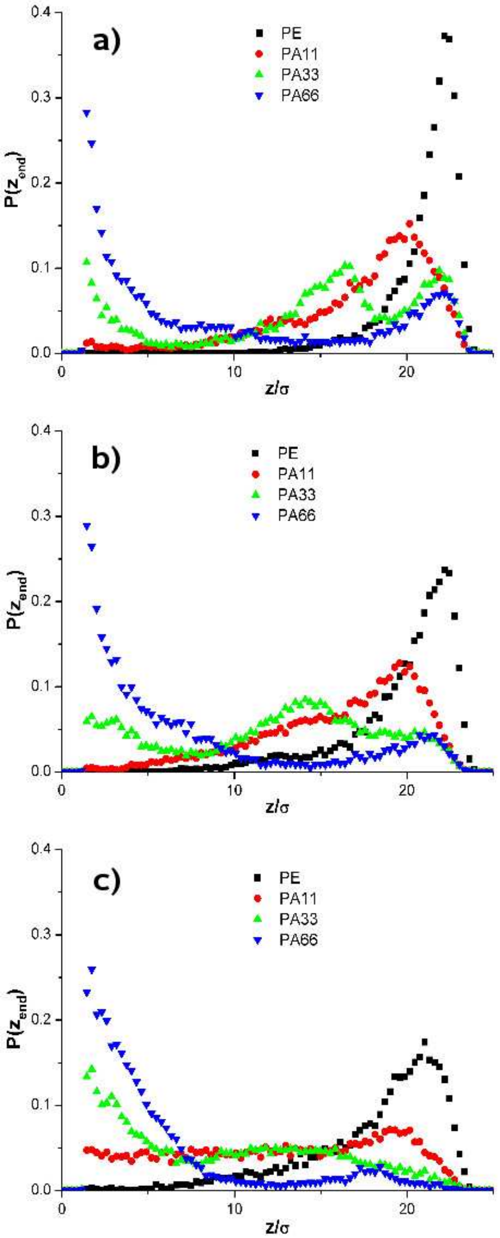

FIG. 5: The histogram of the average distance of the end monomers of the chains from the grafting surface for brushes formed by PE, PA11, PA33 and PA66 chains at grafting densities a) $\rho_a\sigma^2 = 0.1$, b)$\rho_a\sigma^2 = 0.06$ and c) $\rho_a\sigma^2 = 0.02$.

In the case of the brushes of polyampholyte chains, the net charge of the brush layer is zero and most of the counterions are outside the brush. The average thickness in this case has a considerable dependence on the grafting density and the interaction between the anchored chains. At each value of the grafting density, brush thickness decreases with increasing the length of the blocks of similarly charged monomers. Also, as it can be seen in Fig. 3, the average thickness of the brushes formed by the chains with longer blocks of similarly charged monomers has stronger dependence on the grafting density (see growing slope of $\frac{\langle z_m \rangle}{\sigma}$versus $\rho_a\sigma^2$ from PA11 to PA66).

To describe such dependence of the brushes thickness on the grafting density it is instructive to study the equilibrium statistics of conformations of the chains. Accordingly, we monitor the histograms $P(R)$ and $P(z_{end})$ which are defined in Sec. II in our simulations. In Figs. 4 and 5 the histograms $P(R)$ and $P(z_{end})$ at three different grafting densities are shown for brushes of polyelectrolyte and three different polyampholyte chains. It can be understood from Figs. 4 and 5 that decreasing the average thickness of a polyampholyte brush with increasing the length of the blocks of similarly charged monomers originates from two different mechanisms at low and high grafting densities. At low grafting densities, the anchored chains both in polyelectrolyte brush and in three different polyampholyte brushes have stretched conformations and the average end-to-end distance, R, has its maximum value in most of equilibrium configurations (see Fig. 4 c). In Fig. 5 c, the histogram $P(z_{end})$ shows that at such low values of the grafting density the polyelectrolyte brush is aligned and the PE chains are mostly perpendicular to the grafting surface. In this figure, it can be seen that in the case of polyampholyte brushes with long blocks of similarly charged monomers, $z = 0$ part of $P(z_{end})$ is nonzero and increases with increasing the length of blocks of similarly charged monomers. From these two histograms one can conclude that in the brushes of polyampholytes with long blocks of similarly charged monomers, PA33 and PA66, the chains have rod-like conformations and fluctuate in the vicinity of the grafting surface. Snapshots of the brushes of these chains (not shown here) show that the chains are linked to each other as doublets near the grafting surface because of the strong electrostatic attractions. In the case of the brush of PA11 chains, the end monomers of the chains have a uniform distribution inside the brush. In this case, electrostatic neutrality is satisfied in smaller length scales and the electrostatic correlations between the chains are very weak.

At high grafting densities, the histogram of the average end-to-end distance of the chains shows that in the brushes of polyampholyte chains consisting of long blocks of similarly charged monomers, despite the case of low grafting density, the chains tend to have buckled conformations. The histogram of the average z component of the end monomers, $P(z_{end})$, shows two maximums around $z = 0$ and $z = L$ in the case of the brush of diblock PA66 chains and three maximums in the case of the brush of PA33 chains. The energy needed for buckling a semiflexible chain ($L_c \sim l_p$), E_b, is of the order of thermal energy, k_BT. In dense brushes of the chains PA33 and PA66, blocks of similarly charged monomers of the chains form highly charged layers of monomers which produce strong electrostatic field. When the electrostatic energy of similarly charged monomers of the end blocks of the chains due to the electric field of the layer of opposite charge exceeds the bending energy, $E_b \sim k_BT$,

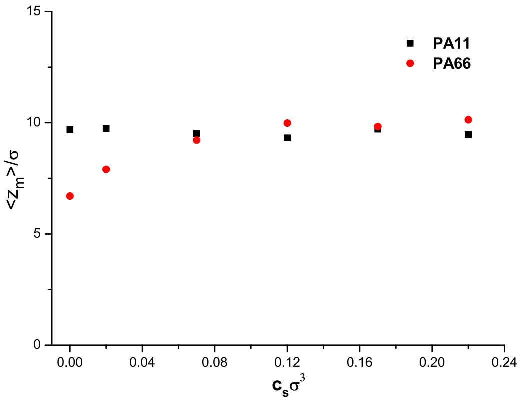

FIG. 6: Salt concentration dependence of the average thickness of brushes of PA11 and PA66 chains at grafting density $\rho_a\sigma^2 = 0.08$. As it can be seen, the thickness of the brush formed by the chains with long blocks of similarly charged monomers is an increasing function of the salt concentration. The size of the symbols corresponds to the size of error bars.

the chains buckle toward the grafting surface. For example, in the case of the brush of diblock PA66 chains, the electrostatic energy of positively charged monomers of each chain roughly can be written as $E_{el} \simeq \frac{fNe}{2} E \frac{L}{2}$ in which $E = 4\pi\rho_a e/\varepsilon = 4\pi k_B T l_B \rho_a/e$ is approximately the electric field of the layer of anchored blocks of negatively charged monomers. With parameters that we use in our simulations, at high grafting densities of the brushes formed by PA33 and PA66 chains, $E_{el} > k_B T$ and buckling of the chains is expected. In the case of the brush of PA66 chains, two maximums in the histogram $P(z_{end})$ shows that buckled chains and those that are straight and perpendicular to the grafting surface coexist. In the brush of PA33 chains, there are two layers of negatively charged monomers and considering the chains of straight configuration, three maximums seen in the histogram $P(z_{end})$ is expected.

The effect of added salt on the brushes of polyampholyte chains is also studied using explicit monovalent salt ions. We observe that properties of the brushes formed by the chains containing longer blocks of similarly charged monomers are more sensitive to the salt concentration. The average thickness of these brushes at all grafting densities increase with increasing the salt concentration and reach to its maximum value (see Fig. 6). This behavior is completely different from that of a polyelectrolyte brush which its thickness is known that decreases with increasing the salt concentration. In the case of a polyelectrolyte brush the electrostatic repulsion between the chains tend to swell the brush and the screening effect of added salt decreases the average brush thickness. However, in the case of the brush of polyampholyte chains with long blocks of similarly charged monomers, the electrostatic interactions between the chains are attractive and tend to decrease the brush thickness. In these brushes, electrostatic screening of the salt ions increases the average thickness. It also can be seen in Fig. 6 that the added salt doesn't change the average thickness of the brush of PA11 chains in which because of local electrostatic neutrality the electrostatic correlations are negligible. In Fig. 7 the equilibrium histograms $P(R)$ and $P(z_{end})$ for the brush of PA66 chains are shown at different salt concentrations. It can be seen that with adding more salt to the system, the chains become more straight (see part b of the figure) and $z = 0$ part of the histogram $P(z_{end})$ vanishes which means that the brush becomes more aligned.

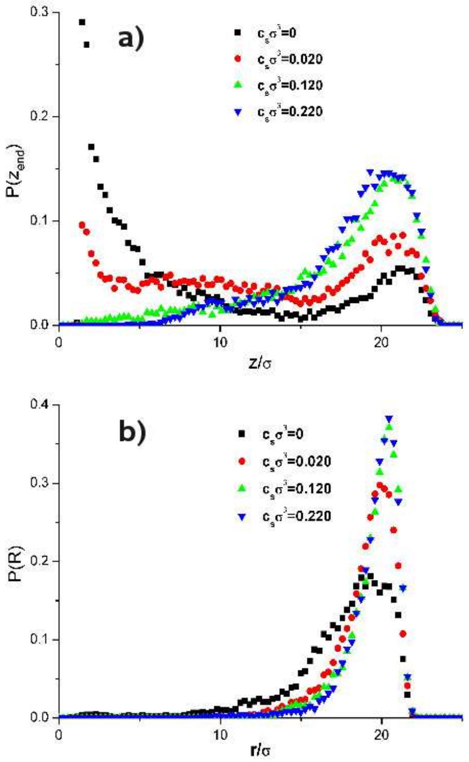

FIG. 7: Histograms a)$P(z_{end})$ and b)$P(R)$ for the brush formed by PA66 chains at different salt concentrations. The grafting density is $\rho_a\sigma^2 = 0.08$.

To estimate the importance of finite size effect in our simulations, we calculated equilibrium average of l_{lat} (defined in Sec. II) for the brush of PA66 chains at highest grafting density $\rho_a\sigma^2 = 0.1$ and found that $\langle l_{lat}\rangle \simeq 11.7\sigma$. The fact that the value of $\langle l_{lat}\rangle$ is less than the lateral box length, $L \simeq 16\sigma$, means that the chains doesn't overlap with their own images in our simulations. We also repeated the simulation of the PA66 brush at grafting density $\rho_a\sigma^2 = 0.1$ with $M = 64$ chains (instead of $M = 25$) and didn't obtain different results.

IV. DISCUSSION

Osmotic pressure of trapped counterions inside polyelectrolyte brush in the osmotic regime is one of the main factors determining the equilibrium brush thickness. Nonetheless, because of the electrostatic neutrality of the chains, Gouy-Chapman length diverges in the case of polyampholyte brushes considered in this paper and most of counterions are outside the brush layer (see Fig. 2 b, c and d). These counterions have no rule in the equilibrium brush thickness. In this case the brush thickness is resulted from the interplay between inter- and intra-chain electrostatic attraction of oppositely charged blocks, inter-chain excluded volume interactions and the bending elasticity of the chains. Hence, dependence of the average thickness of such polyampholyte brushes on the grafting density is of quite different mechanism. However, it is interesting that this dependence is still linear similar to that of a polyelectrolyte brush (see Fig. 3). This dependence in brushes of polyampholyte chains with long blocks of similarly charged monomers is appreciably stronger than the case of polyelectrolyte brush (for example in Fig. 3 the slopes of dotted and dashed lines are 16.7 and 40.2 respectively). An important parameter in a brush of semiflexible polyampholytes is the bending rigidity of the chains, k_{bend}. With decreasing the value of k_{bend}, electrostatic attractions dominate over the chains stiffness and in competition with excluded volume effects determine the average brush thickness. The opposite extreme is the case of the brush of rod-like polyampholytes in which electrostatic correlations can not buckle the chains. So, different regimes corresponding to different values of k_{bend} should be investigated [39].

V. SUMMARY

In summary, we have used molecular dynamics simulations to study planar brushes formed by semiflexible polyelectrolytes and polyampholyte chains with different sequences of charged monomers at various grafting densities and salt concentrations. It has been shown that at grafting densities corresponding to the osmotic regime of the polyelectrolyte brush, the average brush thickness is a weak linear function of the grafting density in agreement with predictions of ref. [23]. The average thickness and equilibrium properties of the polyampholyte brushes have considerable dependence on the grafting density and the salt concentration. This dependence is stronger for brushes of polyampholyte chains containing longer blocks of similarly charged monomers. In brushes of polyampholyte chains with long blocks of similarly charged monomers, at low grafting densities the electrostatic attractions link the chains to each other in the vicinity of the grafting surface and collapse the brush. At high grafting densities, the electrostatic correlations dominate over the bending rigidity of the chains and cause them to buckle toward the grafting surface. Despite the case of polyelectrolyte brushes, the average thickness of polyampholyte brushes with long blocks of similarly charged monomers increases with increasing the salt concentration.

We are grateful to A. Naji, R. Golestanian and F. Mohammad-Rafiee for useful comments and discussions.

[1] Y. Hong, R. L. Legge, S. Zhang, P. Chen, Biomacromolecules. **4**, 1434 (2003).

[2] S. Jun, Y. Hong, H. Imamura, B.-Y. Ha, J. Bechhoefer, P. Chen Biophys. J. **87**, 1249 (2004).

[3] R. Messina Eur. Phys. J. E **22** , 325 (2007).

[4] A. V. Dobrynin, R. H. Colby, M. Rubinstein, J. Polym. Sci., Part B: Polym. Phys. **42**, 3513 (2004).

[5] J. B. Imbert, J. M. Victor, N. Tsunekawa, Y. Hiwatari, Phys. Lett. A **258**, 92 (1999).

[6] A. Baumketner, H. Shimizu, M. Isobe, Y. Hiwatari, J. Phys.: Condens. Matter **13**, 10279 (2001).

[7] Z. Wang, M. Rubinstein, Macromolecules **39**, 5897 (2006).

[8] M. Castelnovo, J. F. Joanny, Macromolecules **35**, 4531 (2002).

[9] N. P. Shusharina, E. B. Zhulina, A. V. Dobrynin, M. Rubinstein, Macromolecules **38**, 8870 (2005).

[10] G. Z. Zheng, G. Meshitsuka, A. Ishizu, J Polym Sci Part B, Polym Phys **33**, 867 (1995).

[11] G. Ehrlich, P. Doty, J Am Chem Soc **76**, 3764 (1954).

[12] C. L. McCormick, L. C. Salazar, Macromolecules **25**, 1896 (1992).

[13] J. M. Corpart, F. Candau, Macromolecules **26**, 1333 (1993).

[14] C. M. Wijmans, E. B. Zhulina, Macromolecules **26**, 7214 (1993).

[15] E. Lindberg, C. J. Elvingson, Chem. Phys. **114**, 6343 (2001).

[16] J. Klos, T. Pakula, Macromolecules **37**, 8145 (2004).

[17] A. S. Almusallam, D. S. Sholl, Nanotechnology **16**, S409 (2005).

[18] P. Pincus, Macromolecules **24**, 2912 (1991).

[19] E. B. Zhulina, O. V. Borisov, Macromolecules **29**, 2618 (1996).

[20] E. B. Zhulina, J. K. Wolterink, O. V. Borisov, Macromolecules **33**, 4945 (2000).

[21] O.V. Borisov, T.M. Birstein, E.B. Zhulina, J. Phys. II **2**, 63 (1992).

[22] E.B. Zhulina, O.V. Borisov, J. Chem. Phys. **107**, 5952 (1997).

[23] A. Naji, R.R. Netz, C. Seidel Eur. Phys. J. E. **12**, 223 (2003).

[24] H. Ahrens, S. Forster, C.A. Helm, N.A. Kumar, A. Naji, R.R. Netz, C. Seidel J. Phys. Chem. B **108**, 16870 (2004).

[25] A. Naji, C. Seidel, R.R. Netz Adv. Polym. Sci. **198**, 149 (2006).

[26] F. S. Csajka, C. Seidel, Macromolecules **33**, 2728 (2000).

[27] C. Seidel, Macromolecules **36**, 2536 (2003).

[28] H. Fazli, R. Golestanian, P. L. Hansen, M. R. Kolahchi, Eur. Phys. Lett **73**, 429 (2006).

[29] O.V. Borisov, T.M. Birstein, E.B. Zhulina, J. Phys. II **1**, 521 (1991).

[30] N. P. Shusharina, P. Linse, Eur. Phys. J. E **4**, 399 (2001).

[31] N. P. Shusharina, P. Linse, Eur. Phys. J. E **6**, 147 (2001).

[32] A. Akinchina, N. P. Shusharina, P. Linse, Langmuir **20**, 10351 (2004).

[33] A. Akinchina, P. Linse, Langmuir **23**, 1465 (2007).

[34] P. Linse, J. Chem. Phys **126**, 114903 (2007).

[35] H.J. Limbach, A. Arnold, B.A. Mann and C. Holm, Comp. Phys. Communications **174**, 704 (2006).

[36] G.S. Grest and K. Kremer, Phys. Rev. A **33**, 3628 (1986).

[37] R. Strebel, R. Sperb, Mol. Simul. **27**, 61 (2001).

[38] A. Arnold, C. Holm, Comput. Phys. Commun. **148**, 327 (2002).

[39] M. Baratlo, H. Fazli (unpublished).